COINCIDENCE PROBABILITIES FOR A NETWORK OF INTERFEROMETRIC DETECTORS OF GRAVITATIONAL WAVES

Massimo Tinto

Department of Applied Mathematics & Astronomy
University College, Cardiff CF1 1XL, Wales UK

LIGO-T870006-00-R

Summary

The coincidence probabilities for a network of Laser Interferometric Gravitational-Wave detectors, observing bursts from coalescing binary systems containing neutron stars or black holes, are calculated by developing the theoretical results deduced in a previous paper. After deriving the formula for the single-detector *antenna pattern* n for plane-waves from binaries, we calculate the single-detector detection probability as well as double, triple and quadruple coincidence rates for likely detector locations in USA and Europe. We find that proposed detectors would be able to see events from sources out to 550 Mpc with a probability greater than 80% when working at their expected sensitivities.

In coincidence experiments with two, three or four detectors the coincidence probabilities decrease to a typical value of 70% for double coincidences, 63% for triple and 57% for quadruple. This allows us to calculate the mean number of coincidences per unit time for coalescing compact binaries out to a given distance.

1. Introduction

Since the early experiments of Joseph Weber at the University of Maryland, work on gravitational wave detectors has long been motivated by the expectation that supernova explosions are the most important and interesting events for the detectors to see. While these may still prove to be important sources, there is still great uncertainty about the likely strength of the waves they produce. In recent years a new class of gravitational wave source has begun to occupy a central place in the thinking of experimental and theoretical relativists: the coalescences of compact binaries (containing neutron stars or black holes). They were first discussed by Clark and Eardly (1977), but it was Kip Thorne who first pointed out their importance for broad-band Laser Interferometric Gravitational-Wave Observatories (LIGOs).

Although possibly weaker than the waves from supernovae, those from coalescing binaries have a unique signature that enables them to be extracted from wide-band data by digital filtering techniques (see Thorne 1987, Schutz 1986, Dewey 1986). This signature is their accelerating sweep upwards in frequency as the binary orbit decays. Since the signal from a supernova is short-lived (and hard to predict), coalescing binaries have the advantage over supernovae in signal-to-noise ratio by a factor depending on the square-root of the ratio between the corresponding number of cycles in the wave trains (see Thorne, 1987). This is in fact the enhancement in effective signal that the experimenters will achieve by optimal signal processing in their search for these frequency-sweeping bursts. The key to being able to take advantage of this is the confidence with which we can predict the wave form. Because the binary system spends more time in the low-frequency part of the sweep than in the high-frequency part or in the final

coalescence, and because gravity wave detectors have less amplitude noise at low frequencies (~100 Hz) than at high (>100 Hz) (see Hough *et al.*, 1986), it will be easier for detectors to see the Newtonian regime of the sweep than the post-Newtonian one. In the Newtonian regime, if we orient the wave's polarization axes along the axes of the projection of the orbital plane on the sky, then the wave's amplitudes assume the following form, (units: c = G = 1)

$$h_+ = 2(1+\cos^2 i)(\mu/r)(\pi M f)^{2/3}\cos(2\pi f t) \qquad (1.1)$$

$$h_\times = \pm 4\cos i\,(\mu/r)(\pi M f)^{2/3}\sin(2\pi f t) \qquad (1.2)$$

where i is the angle of the inclination of the orbit to the line-of-sight of the detector; M and μ are the total and reduced masses, r the absolute distance to the binary and f the frequency of the waves (equal to twice the orbital frequency), (see Thorne, 1987).

From a study of the wave form (1.1,2) by using a network of broad-band detectors located at different places on the Earth, we can in principle deduce the following information: (i) the direction to the source; (ii) the inclination of the orbit to the line-of-sight; (iii) the direction the stars move in their orbit; (iv) the combination $\mu M^{2/3}$ of the reduced and total masses; (v) the distance r to the source. In particular in coincidence experiments with four detectors it would be possible to test Einstein's predictions regarding gravitational wave polarization: four detections over determine the solution for a transversely polarized quadrupole wave, so any inconsistency among the data would be evidence for other polarization states. Besides this important point, Schutz (1986) has shown from a detailed analysis of the expected noise in future LIGOs that it would be possible to obtain a significantly better value for the Hubble constant than now we have.

Although it is possible to predict the shape of the

signal with great confidence, there is considerable uncertainty about the rate of coalescence events. Clark, van den Heuvel and Sutantyo (1979) have estimated, from neutron star observations in our own galaxy, that to see three coalescences of neutron-star binaries per year one must look out to a distance of ~100 Mpc. Recent improvements in the statistics of neutron star binaries reinforces this conclusion but, at the same time, shows that this number might be drastically changed by plausible astrophysical scenarios. In what follows we shall adopt the figure of three per year out to 100 Mpc, bearing in mind its uncertainty.

In this paper we shall calculate the coincidence probabilities for a network of Interferometric detectors observing bursts from coalescing compact binaries, by extending the investigation begun in the previous papers by Schutz & Tinto (1987) and Tinto (1987), referred to as paper I and II respectively. In I we deduced a remarkable relationship between the geometrical factors affecting the responses of two detectors working in coincidence and their thresholds.

We proved that the mean overlap of the squared modulus product of two different antenna patterns equals the average of the coincidence probability C over all thresholds. By studying the geometrical properties of this function for several pairs of likely detector locations we deduced values for the orientations of the instruments that maximize mean coincidence rates and we showed that these angles are insensitive to whether the wave is linearly or elliptically polarized, (see for details I and II). In paper I we pointed out that the *mean* coincidence probability, defined as the average of the coincidence probability over all thresholds, does not give a fair indication of the typical probability for two detectors of registering

the same burst. The concidence probability depends on the thresholds of the instruments. In this paper we shall develop an algorithm for calculating the full coincidence probability for broad-band detectors, at several widely spaced locations on the earth, as a function of their thresholds relative to the amplitude of the wave. Here we briefly summarize our method.

In §2 we write the analytical expression for the *antenna pattern* η for waves from coalescing compact binaries. This function depends on the source angle $(\theta;\phi)$, the polarization angle of the wave ψ, the inclination i of the angular momentum of the binary to the line-of-sight of the detector and the angles $(\alpha;\beta;\gamma)$ representing the orientation, latitude and longitude of the detector.

After recalling the theorem proved in paper I for the mean coincidence probabilities (eq.(2.8) below), we point out that future LIGOs would be able to see coalescing compact binaries with signal-to-noise ratios large enough to enhance considerably the real coincidence probabilities with respect to the corresponding mean values calculated in I and II.

In §3 we evaluate the single-antenna detection probability as well as the double, triple and quadruple coincidence rates in terms of the detectors' thresholds relative to the amplitude of the wave. We take 4 detectors in their proposed locations: California, Maine, Scotland and Bavaria. A fifth detector may be built in France, but we do not include that here. We find that in the expected range of thresholds triple coincidence probabilities follow reasonably well double coincidence rates but are about 10% below them, and that quadruples similarly follow triples with a further drop of around 5%. Physically this is due to the fact that the two European detectors will lie on roughly the same tangent plane to the earth. Therefore, a trans-

atlantic double coincidence will usually be a triple and a coincidence involving the two American detectors and one European one will generally involve the fourth detector as well. In §4 we discuss the result and conclude that a network of four large-scale laser interferometric gravitational wave detectors, working at their optimum sensitivites, will have a probability greater than 50% of detecting simultaneously bursts from compact-neutron-star binaries out to 550 Mpc.

2. Antenna patterns for waves from a binary system

The response of an interferometric detector of gravitational waves consists basically of the change $\delta\ell/\ell_o$ in the relative length of the two arms. Its analytical expression has been deduced in I for plane waves and in the long-wavelength approximation (reduced wavelength $\lambda/2\pi \gg$ arm-length ℓ_o). The general expression may be written as follows:

$$\frac{\delta\ell}{\ell_o} = \sin 2\Omega \left[E(\alpha;\beta;\gamma-\phi;\theta;\psi) h_+ + E(\alpha;\beta;\gamma-\phi;\theta;\psi+45^\circ) h_\times e^{j\zeta} \right]. \qquad (2.1)$$

where j is the imaginary unit.

For a derivation of the function E, its properties and a complete description of the geometry involved we refer the reader to §(2-3) of I. Here we only point out that:

i) 2Ω is the angle between the two arms of the interferometer (see Figure 1);

(ii) the parameters α, β and γ are respectively the angle between the direction of the detector bisector and the local meridian, the latitude and longitude of the detector on the Earth (see Figures 1-2);

(iii) (θ,ϕ) and ψ are associated, respectively, to the direction of the incoming wave and the inclination of the

axes of the polarization ellipse.

(iv) h_+ and $h_\times$ are the amplitudes of the two independent polarization states (referred to the orientation angle ψ), and ζ is the phase lag of one polarization with respect to the other.

If the wave is radiated by a coalescing compact-binary, the wave's two amplitudes h_+, $h_\times$ and their relative phase ζ may be written as follows in the Newtonian approximation: (Thorne, 1987)

$$\zeta = \pm \frac{\pi}{2} \; ; \; h_+ = \frac{1}{2}(1+\cos^2 i)h; \quad h_\times = \cos(i)h \qquad (2.2)$$

where i is the inclination of the angular momentum of the source to the line-of-sight of the detector and h is equal to:

$$h = 4 \left[\frac{\mu}{r} \right] \left[\pi M f \right]^{2/3} \qquad (2.3)$$

where M and μ are the total and reduced masses, r the absolute distance to the binary and f the frequency of the wave (Thorne, 1987). Notice that h is the maximum possible amplitude one can receive from the source; for most events, the angular factors in Eq. (2.2) will reduce the observed amplitude below h. From Eq. (2.2) we easily deduce the following form for the *antenna pattern* n:

$$n = \frac{\delta\ell}{\ell_o h} = \sin 2\Omega \left[\frac{E}{2}(1+\cos^2 i) \pm j \cos i \, \bar{E} \right] \qquad (2.4)$$

where we have denoted with $\bar{E}$ the function $E(\alpha;\beta;\gamma-\phi;\theta;\psi+45^\circ)$.

The size of the detector's response depends not only on the geometrical factors mentioned in points (ii) and (iii) but also on the level of noise and its statistical distribution. In practice a variety of noise sources will set an effective threshold $(\delta\ell/\ell_o)_*$ on the level of response

$\delta\ell/\ell_0$ that can reliably be distinguished from noise during a given observation time. According to the hypothesis made in I, we shall assume that any $(\delta\ell/\ell_0)$ larger than $(\delta\ell/\ell_0)_*$ is detected *and any* smaller one is lost.

In paper I we have been able to prove a relationship between the geometrical factors affecting the response of the detector and its thresholds relative to the amplitude of the wave. Here we only summarize the main results while for a full proof and analysis we refer the reader to I.

Over a large number of observations we can expect the time of arrival and polarization angle of the gravitational waves to be random. We may therefore take the angles Φ and Ψ to be random variables uniformly distributed on the interval $(0, 2\pi)$ and calculate the following expectation values:

$$\langle X\rangle, \quad \langle X_1, X_2\rangle \tag{2.5}$$

where $X = |\delta\ell/\ell_0 h|^2$ is the *antenna's power pattern*, the angle brackets denote averages over random variables, and the indices 1, 2 refer to different detectors. We shall discuss below how these quantities should be interpreted in order to get meaningful information about coincidence experiments.

Independent detections of any given gravitational wave event by different detectors is vital for its reliable identification as a gravitational wave. This is because the events may not be much larger than the noise level. In white-Gaussian noise, the type of noise expected at the output of a shot noise limited interferometric antenna, a 5σ excursion will be likely once in every 17×10^6 sampling times. For coalescing compact binaries the sample time is of the order of 10 millisecond, so 5σ events occur 5 times a day. Coalescences of neutron stars out to 500 Mpc occur 5 times a week or so, and may not be more than 5σ in amplitude for the proposed detectors. More detectors will lower the

rate of noise events. Two detectors will have 5σ coincidences within a 40 sampling-time window (to allow for time delays as the wave travels from one detector to another) once every 7×10^{10} sampling times. This corresponds to about 2 noise events per year, allowing events closer than 2Gpc to be reliably identified if they occur at the *predicted rate*. Extra detectors could be built on the same site to gain this advantage, but by spacing them out across the globe one automatically gains much more information, such as the direction to the source.

The probability of coincident observations of a given event depends not only on the geometrical factors but also on the thresholds of the detectors relative to the amplitude of the wave. Let X_* be therefore the threshold of the squared modulus amplitude, the minimum detectable value of $|\delta\ell/\ell_0 h|^2$. For a given h the detection probability of a single antenna is:

$$S(X_*) = \int_{X>X_*} \frac{1}{4\pi^2}\, d\Phi d\Psi \tag{2.6}$$

and the coincidence probability is therefore equal to:

$$C(X_{1*};X_{2*}) = \int_{\substack{X_1>X_{1*}\\ X_2>X_{2*}}} \frac{1}{4\pi^2}\, d\Phi d\Psi \tag{2.7}$$

where the integrals are extended over the region of the (Φ,Ψ) space in which the antenna's power patterns are simultaneously greater than their corresponding thresholds. In I we proved that the mean value of C, over all possible thresholds, is equal to the mean overlap of the antenna power patterns $\langle X_1X_2\rangle$, that is:

$$\langle X_1X_2\rangle = \int_0^1\int_0^1 C(X_{1*};X_{2*})dX_{1*}dX_{2*} \tag{2.8}$$

where the limits of integration are the extreme values that

the thresholds can take. It was therefore possible to extract meaningful information about coincidences by plotting this as a function of the detector orientations, for several pairs of likely locations, for incoming waves from a fixed source as well as from randomly distributed sources on the sky (see diagrams in I and II).

This function tells us how we should orient two detectors sited in two different places in order to maximize the chance of coincidence but does not contain quantitatively exact information of the probability itself. The values of the function $\langle X_1 X_2 \rangle$ that we plotted in I and II are typically 5 to 10%, which might suggest that the probability of a coincidence for two detectors is very small. This is not correct, however. We recall that $\langle X_1 X_2 \rangle$ is a mean value and that the real coincidence probability depends on the thresholds X_{1*} and X_{2*}. Thresholds near zero mean that the signal is strong relative to the noise level, and it will therefore be detectable almost regardless of what direction it comes from. Thresholds near 1, on the other hand, are weighted strongly in the right-hand side of Eq. (2.8) and they mean that the signal is relatively weak; it will be detectable only in a narrow range of incoming directions and polarizations. Since the signal strength, at frequency f, from a binary system of total mass M, reduced mass μ, at a distance r, is:

$$h = 5.5\cdot 10^{-23}\left[\frac{100\text{Mpc}}{r}\right]\left[\frac{M}{M_\odot}\right]^{2/3}\left[\frac{\mu}{M_\odot}\right]\left[\frac{f}{100\text{Hz}}\right]^{2/3} \qquad (2.9)$$

($M_\odot$ is the mass of the sun), and the amplitude noise for a 1 km antenna, working with light recycling (see Hough *et al.*, 1986), is equal to:

$$\sigma = 6.6\ 10^{-25}\left[\frac{f}{100\text{Hz}}\right]^{11/6}\left[\frac{M}{M_\odot}\right]^{1/3}\left[\frac{\mu}{M_\odot}\right]^{1/2} \qquad (2.10)$$

we deduce that with a threshold at 5σ, at 100 Hz and for a binary composed of two 1.4 $M_\odot$ neutron stars, a detector with a 1 km arm-length (as the one proposed by the research group in Glasgow) could see to 550 Mpc with a value of X_{2*}^{M}(= 5σ/h) of about 0.25. In such a case the thresholds are in a range where the coincidence probabilities are highest. The average in Eq.(2.8) therefore weights low coincidence probabilities too strongly for this case. We can expect that our calculations of real coincidence probabilities will yield values much larger than the mean for interesting cases.

We observe that the figure given above of 550 Mpc, for a 20σ observation in a 1 km antenna, disagrees with that used in the literature (Hough *et al.*, 1986; Schutz, 1986) where a value of 100 Mpc at the same level of signal has been assumed. The reason of this is because we are normalizing to the maximum wave amplitude h rather than to its averaged value over detector and source orientations.

3. Coincidence Experiments

(a) Coincidence Probabilities

Over a sequence of observations, besides the arrival time-angle Φ and the polarization angle Ψ of the wave, also the inclination i of the orbit to the line-of-sight of the detector and the azimuthal angle Θ can be considered random variables uniformly distributed over the sphere. This implies the following expression for the coincidence probability, in terms of the thresholds of a network of n detectors:

$$C(X_{1*};X_{2*};\ldots;X_{n*}) = \int_{\substack{X_1>X_{1*}\\ X_2>X_{2*}\\ \vdots\\ X_n>X_{n*}}} \frac{1}{16\pi^2}\sin i \sin\Theta\, d\Theta d\Phi d\Psi di \qquad (3.1)$$

where the integral is over the domain in which the Xs exceed their corresponding thresholds simultaneously. We remind the reader that in Eq.(3.1) we have to limit the orientation freedom of the detectors in some way, otherwise coincidence-rate calculations would have too many independent variables to be tractable. We do so by fixing the orientations on the values that optimize the mean coincidence probabilities. In II we showed that the orientations optimizing simultaneously double, triple and quadruple mean coincidence rates are essentially independent of the type of polarization of the wave.

Because of the multidimensional nature of the integrals that we want to calculate, and the complexity of the domain of intergration, we have used the Monte Carlo method. For a full description of this method we refer the reader to Shreider (1966). Here we briefly summarize its main features relevant to our problem by a fairly simple example.

Let us assume that we have to calculate the surface area Γ of a certain plane figure S. It may be a completely arbitrary figure with curvilinear boundary whether it be connected or consisting of several sections, and specified graphically or analytically. Let us assume that it is enclosed within a unit square. Suppose that we choose a random point in the square by taking one whose coordinates are independently uniformly distributed in the interval (0,1). It is clear that the probability for this point to lie in the region S is equal to Γ. By applying the large-number's theorem we may give an approximate estimate of the area Γ.

Let us select N random points, uniformly distributed

inside the unit square. Let N′ designate the number of points that happened to fall within S. We have that the ratio N′/N gives an estimate of the area that we want to calculate. The greater N the higher the accuracy of the estimate. In order to evaluate the precision of this estimate we may use the central limit theorem in the following form (see Shreider, 1966):

$$P\left\{|N'/N - \Gamma| < \epsilon\right\} > 1 - \frac{\Gamma(1-\Gamma)}{\epsilon^2 N} > 1 - \frac{1}{4\epsilon^2 N} \qquad (3.2)$$

that is, the probability of evaluating Γ within an error ϵ is greater than a quantity depending on the number of trials N and ϵ itself. Setting for a given ϵ a guaranteed probability in the following way:

$$P\left\{|N'/N - \Gamma| < \epsilon\right\} > 1-\delta \qquad (3.3)$$

we obtain from the inequality (3.2) that the condition (3.3) is verified *a priori* if we have:

$$\delta = \frac{1}{4\epsilon^2 N} \qquad (3.4)$$

In other words the precision of our estimate is inversely proportional to the square-root of the number of trials:

$$\epsilon = \frac{1}{2\sqrt{\delta N}} \qquad (3.5)$$

We observe that this is an upper limit to the error ϵ and we should remember this fact when discussing the calculations for the coincidence probabilities.

From the central limit theorem (Eq.(3.2)) we may conclude that the number of trails N does not depend on the dimensions of the integral. Therefore the utilization of the Monte Carlo method is advantageous in calculating multiple integrals, as against the use of quadrature formulas which involves great difficulties. The principal

feature of the Monte Carlo method in our problem is in fact the simple structure of the computation algorithm. As a rule, a program is prepared to perform only one random trial, that is to select a random point within the limits of a certain region and check whether it lies within the domain of intergration. This trial is repeated N times, each trial being independent of all others, and the results of all trials are averaged.

(b) Probability of Detection for a single-Antenna

If we assume n = 1 in Eq.(3.1) we obtain the expression of the detection probability for a single antenna with threshold $X_\sharp$:

$$S(X_\sharp) = \int_{X>X_\sharp} \frac{1}{16\pi^2} \sin i \sin\theta \, d\theta d\phi d\Psi di \qquad (3.6)$$

Since we are averaging over all possible directions and polarization states of the incoming wave, the result will not be affected by the particular location and orientation of the antenna.

The calculation of the integral (3.6) and of the appropriate integrals for the double, triple and quadruple coincidence rates, has been done on the ICL-3980 of the South West University Regional Computer Centre by using the NAG library for generating uniformly distributed random numbers and assuming the number of trials N equal to 10^4. If we use Eq.(3.4) for the error ϵ, by fixing δ to 10^{-2} and N to 10^4 we deduce an error of 5%. In other words the probability of obtaining a result affected by an error smaller than 5% is greater than 99%. We shall see later that the choice we have taken for N provides consistent results.

In Figure 3 we plot the detection probability against

the detector's thresholds relative to the amplitude of the wave. As expected this is a decreasing function of $X_\sharp^{1/4}$, going from 1 to zero as $X_\sharp^{1/4}$ get from zero to 1.

For a single-detector experiment, it is more likely that the experimenters will fix the threshold on 7σ than 5σ in order to minimize the number of Gaussian fluctuations against the rate of burst events of likely amplitudes. In this assumption we may convert our variable $X_\sharp^{1/4}$ into the more usual signal-to-noise ratio (SNR) simply by replacing $X_\sharp^{1/4}$ with $7X_\sharp^{-1/4}$. From the considerations made in §2 on the predicted noise and wave amplitudes for LIGOs observing coalescing binaries, we have that the interesting interval for the $X_\sharp^{1/4}$s is between 0.15 and 0.50. In terms of SNR this means between 14 and about 45. At SNR 14 the single antenna probability is equal to 20%; increasing the SNR to the value of 25 the probability goes up to 55%. For SNRs greater than 40, which in principle may be achieved by an optimum combination of higher laser power, better and heavier mirrors, longer baselines, active seismic isolation and the use of "squeezed states" (see Caves, 1981), we deduce from Figure 3 that the detection probability will be greater than 85%.

For values of $X_\sharp^{1/4}$ in the interval [0, 0.5] we have done a least-squares fit to our data points by using a linear combination of Chebyshev polynomials. This provides a useful way of representing output of these calculations. The reason for preferring such a fit relies on the condition of having independent errors in our data, (see Hamming, 1973). We have used the set of Chebyshev polynomials because, among all other orthogonal polynomials, they minimize the maximum deviation from the data, providing at the same time an expansion with the fastest rate of convergence (see Fox & Parker, 1968). Finally we have chosen the degree of the approximating polynomial by looking at the sign changes in the residuals. If we assume the

residuals to be random and independent of one another, then we should expect to see about half the number of possible sign changes. Within a few times the square-root of this number, we have verified this condition when the degree of the approximating polynomial is two. In the appendix, after extending the least-squares fit to double, triple and quadruple coincidence rates, we provide the coefficients of the corresponding Chebyshev expansions.

(c) Double Coincidence Probabilities

In Figure 4(a-f) we plot contours of constant $C(X_{1\$}^{M}, X_{2\$}^{M})$ for the six independent baselines among California, Maine, Scotland and South Germany. We have left out from our considerations the planned detector in France because it will lie essentially on the same tangent plane containing the Munich instrument and therefore will have the same coincidence rates, when operating in coincidence with any other detector in its optimum orientations.

Figure 4(a-f) shows that the double coincidence probability is symmetric under interchange of its variables $X_{1\$}^{M}$, $X_{2\$}^{M}$:

$$C(X_{1\$}^{M}; X_{2\$}^{M}) = C(X_{2\$}^{M}; X_{1\$}^{M}) \qquad (3.7)$$

This condition, also verified by triple and quadruple coincidence probabilities, is a consequence of having averaged over all directions of the incoming wave. The degree to which the Monte Carlo calculations obeys this symmetry is a measure of their accuracy. The only remaining geometrical factors affecting the coincidence probabilities are the detectors' relative latitude, longitude and the orientations. The effect of the angular separation, in each baseline, on the coincidence probability, appears more clearly for values of the thresholds $X_{\$}^{M}$ greater than 0.25. At $X_{1\$}^{M} = X_{2\$}^{M} = 0.5$ for instance, the coincidence probability goes from 5% for the California-South Germany baseline (Figure 4(c)) to about 17% for the Scotland-South Germany baseline (Figure 4(f)). This value is only 3% smaller than the coincidence probability for two identical detectors sited next to each other (see Figure 3 for the single-detector probability).

As we said earlier, we have fixed the orientations on the values optimizing the mean coincidence rates deduced in I. However for geographic reasons not all detectors will assume the configurations suggested in I. In order to quantify by how much the coincidence probabilties would be reduced by a different choice of the orientations, we have calculated coincidence rates in terms of the detectors' orientations for characteristic thresholds. We have found that for thresholds equal or smaller than 0.20 the coincidence probabilities are not significantly affected by the angles we choose. Physically this is due to the elliptical polarization of the waves.

This should be remembered when a decision for a suitable orientation of the detectors in Germany and France will be taken. By orienting them with 45 degrees of difference, we would be able to get useful information about the degree of elliptical polarization of the wave by looking at the time delay in this baseline (Schutz, 1986).

Before discussing Figure 4(a-f) we recall that in coincidence experiments the noise sources in the detectors will be independent. Therefore we may reduce the threshold levels to 5σ in either instruments (see Hough *et al.*, 1986). Within this assumption the SNR is given by $5X_{\$}^{-M}$.

Figure 4(a) refers to detectors in California ($X_{1\$}^{M}$) and Maine ($X_{2\$}^{M}$). Since current detector designs for these two sites propose a common arm-length of 4 km, we shall comment only on values of the coincidence proabibility

corresponding to the same threshold. For SNRs equal to 10 for both instruments the coincidence probability is about 12%. By increasing the SNRs to 20 the probability goes up to the value of 55%; reaching SNRs 30 the probability is around 75%. For SNRs greater than 40, which proposed LIGOs will probably achieve, the coincidence probability will be above 85%.

Figure 4(b) is for detector 1 in Los Angeles and detector 2 in Glasgow. In this baseline the detector in North America will be in principle more sensitive than the detector in Scotland because of the proposed longer arm-length. Roughly we may predict a ratio of 2 in sensitivity when the detectors are working with light recycling (see Hough *et al.*, 1986). We should therefore focus our attention on values of the coincidence probability on the straight line $X_{2\sharp}^{\flat\flat} = 2X_{1\sharp}^{\flat\flat}$. From the estimate of 0.25 given in §2 for $X_{\sharp}^{\flat\flat}$, in the case of a 1 km detector working with light recycling at 100 Hz and searching for a binary of two 1.4 $M_\odot$ neutron stars at 550 Mpc, we deduce a coincidence probability of about 61% for this baseline.

Figure 4(c) refers to the Los Angeles-Munich baseline. The coincidence probability is not much different (the order of 1%) than that shown in the previous figure for the pair Los Angeles-Glasgow. This is due to the small angular separation between Glasgow and Munich. Current designs for the German detector anticipate an arm-length of 3 km with an included angle of 60°. We should therefore consider this apparatus with an effective arm-length of 2.5 km, in principle 1.6 times more sensitive than the British detector and 1.2 times less than the Americans, when all instruments are working with light-recycling.

Figure 4(d) is for the detectors in Maine ($X_{1\sharp}^{\flat\flat}$) and Scotland ($X_{2\sharp}^{\flat\flat}$). Since the angular separation in this baseline is only about 15 degrees greater than that in the

pair California-Maine, we have a coincidence probability nearly equal to that shown in Figure 4(a), with a maximum discrepancy of about 2%. Namely, at SNRs 10 the probability is 11%, at SNRs 20 is equal to 53% and 75% when SNRs are equal to 30.

Figure 4(e) refers to the baseline Maine ($X_{1\sharp}^{\flat\flat}$) and Germany ($X_{2\sharp}^{\flat\flat}$). The same considerations made for Figure 4(c) apply here and therefore we shall not repeat them.

Figure 4(f) considers the two European detectors: Glasgow ($X_{1\sharp}^{\flat\flat}$) and Munich ($X_{2\sharp}^{\flat\flat}$). Since the angular separation between these two sites is smaller than 20 degrees, the contour plot is nearly equal to the one for two detectors sited next to each other. For instance, at SNRs 10 the Glasgow-Munich baseline shows a coincidence probability of 17% against the value of 20% for two detectors located at the same point on the Earth. For SNRs 20 the probability gets to 61% and goes up to 80% for SNRs 30.

(d) Triple coincidence probabilities

The main reasons for preferring triple coincidences to double are because they give added confidence that an event has occurred and also provide much improved directional information for good SNR. If the events are not corroborated by an electromagnetic detection (optical, X-ray or radio telescopes) this could be crucial. In the case of neutron-star binaries, it may well be possible that a gravitational wave event will be accompanied by an optical activity (Schutz, 1986). However, even if there is an optical activity, an all-sky survey is nearly impossible optically. With three detectors, from the two independent time delays and the three amplitude observations, one has in principle enough information for determining the position of the source in the sky within two separate error boxes, to calculate the two independent polarization amplitudes of the

wave and the phase lag between them.

Since the two European detectors will be relatively close together, they will see mostly the same events. This means that a transatlantic double coincidence probability calculation can roughly be considered as a triple, and a coincidence involving both American detectors and at least one European one will also turn out to be a quadruple. Here and in the next paragraph we only point out a few values for triple and quadruple coincidence rates corresponding to certain combinations of SNRs. We shall reproduce in the appendix the analytical expression of the fits we have done to the full calculations.

Among the four possible triple configurations it appears clear from the geometry, and assuming all detectors with the same thresholds, that the combination Maine ($X_{1\sharp}^{H}$)-Scotland ($X_{2\sharp}^{H}$)-Germany ($X_{3\sharp}^{H}$) is the optimum. For this case, and with $X_{\sharp}^{H}$ equal to 0.5 for all detectors, the coincidence probability is 8%; at $X_{\sharp}^{H}$ 0.25 it goes up to 48% and at $X_{\sharp}^{H}$s equal to 0.125 is about 80%. Assuming all three detectors will be working at their optimum-light recycling configuration and looking for signals of amplitudes greater than 5 times their own rms noise levels, a possible combination of the thresholds corresponding to binaries out to 550 Mpc would be the following: $X_{1\sharp}^{H} = 0.125$, $X_{2\sharp}^{H} = 0.25$ and $X_{3\sharp}^{H} = 0.15$. For this sequence the probability is equal to 63%.

A triple coincidence experiment with detectors in California ($X_{1\sharp}^{H}$), Scotland ($X_{2\sharp}^{H}$) and Germany $X_{3\sharp}^{H}$) gives instead a coincidence rate of 5% when all thresholds are at 0.5. it increases to 44% for $X_{\sharp}^{H}$ 0.25 and is equal to 78% at $X_{\sharp}^{H}$ 0.125. At a working configuration equivalent to the one considered for the triple Maine-Scotland-Germany we have a probability of 60%.

For the combination California ($X_{1\sharp}^{H}$)-Maine ($X_{2\sharp}^{H}$)-Scotland ($X_{3\sharp}^{H}$) the coincidence probability is 4% when the $X_{\sharp}^{H}$ are 0.5; it increases to 43% at $X_{\sharp}^{H}$ 0.25 and goes to 75% at $X_{\sharp}^{H}$ 0.125. The combination $X_{1\sharp}^{H} = X_{2\sharp}^{H} = 0.125$ and $X_{3\sharp}^{H} = 0.25$ gives a coincidence probability of about 59%.

The remaining possible combination, namely California-Maine-Germany, gives the following values for the coincidence rates at equal thresholds: 3% at $X_{\sharp}^{H}$ 0.5; 41% at $X_{\sharp}^{H}$ 0.25 and 74% when the $X_{\sharp}^{H}$s are 0.125. In this triple coincidence we may assume as indicative the following sequence of thresholds: $X_{1\sharp}^{H} = X_{2\sharp}^{H} = 0.125$ and $X_{3\sharp}^{H} = 0.15$. Correspondingly the coincidence rate is 73%.

The figures given above allow us to get an idea about the mean number of coincident detections of coalescing-compact objects in a network of three detectors. Assuming the value of 3 coalescences per year for neutron-star binaries out to 100 Mpc (Clark *et al.*, 1979), we deduce that out to 550 Mpc, and with detectors working at their optimum sensitivities, the *mean number* of triple coincidences would be between 290 and 360 per year.

(e) Quadruple coincidence probabilities

From observations of coalescing binaries with a network of four LIGOs we may obtain a series of astrophysical information of extraordinary relevance.

In a recent paper Schutz (1986) has shown that, by observing a burst from a coalescing compact binary, four detectors of sufficiently large SNRs would allow us to determine to a few per cent the absolute distance to the system and to locate its position in the sky within an error of $\pm 3^{\circ}$. If the coalescence is optically identifiable, then by measuring the redshift we can determine the Hubble constant H_0 to a few percent. Otherwise, combining statistically a reasonable number of events, we can obtain H_0 to

within the same precision.

Detecting the dominant mass-quadrupole radiation allows us to measure the quantity $\mu M^{2/3}$ (Eq.(1.1-2)). If the mass combination $\mu M^{2/3}$ is less than about $2M_\odot^{5/3}$, we can be fairly sure that the binary was made of neutron stars; if it is larger we can be sure that at least one of the bodies was a massive black hole (Thorne, 1987).

A gravitational observation with four detectors would test Einstein's theory of relativity: four detections contain three independent time-delay and four amplitude observations which all together overdetermine the solution for a transversely polarized quadrupole wave. Any inconsistency among them would show different spin properties of the wave.

With our calculation we are able to give an estimate of the chance of recording an event, of a given amplitude, in a network of LIGOs characterized by a suitable combination of thresholds and rms noise levels. The analytical expression for the quadruple coincidence probability provided in the appendix allows us in fact to do so. Here, however, we shall only reproduce a few values corresponding to certain threshold combinations. This should give us an idea about a characteristic range for the coincidence rates.

When all detectors have a X_s^M equal to 0.5 the coincidence probability is about 3%. Reducing by one-half the threshold X_s^Ms the chance of simultaneous detection goes up to 39% and at X_s^Ms equal to 0.125 we get to a coincidence rate of 81%. For the combination of thresholds already mentioned for triple coincidences, that is: California and Maine at X_s^M 0.125, Scotland with X_s^M 0.25 and Germany at X_s^M 0.15 the coincidence probability is 57%, only 6% less than the mean value among the four triple coincidence rates calculated in the previous paragraph for the same thresholds' sequence. In other words any triple coincidence rate

can be considered to be a good representation of a quadruple.

If we look for sources twice as far in distance, this combination of thresholds has to be multiplied by a factor two reducing the detection probability to about 17%. So while at 550 Mpc we have SNR good enough for angular location of the source in the sky (Schutz, 1986) and about 280 coincidence detections per year, smaller SNR raise the event rate by a factor of about 2.5 to 680 coincidences per year.

4. Conclusions

A coincidence experiment with two or more detectors enhances the probability of detection of gravitational bursts because it singles them out from uncorrelated noise pulses. The principal result of this paper has been the calculation of the coincidence probability for a pair, triple or quadruple of laser interferometers widely located on the Earth observing coalescences of compact objects. We found that the network of four planned detectors in USA and Europe, working at their optimum sensitivies, would be able to register a mean number of coincidences of about 280 per year when looking for 1.4 $M_\odot$ neutron-star binaries out to 550 Mpc.

This would allow us a number of astrophysical observations otherwise impossible and a test of Einstein's theory of Relativity.

Acknowledgements

I thank Professor Bernard F. Schutz for several important comments and for his patient and continuous encouragement. I also thank Professor Enrico Massa for a stimulating conversation on the Monte Carlo method. The financial support was provided by the Italian Ministry of Education.

Figure Captions

Figure 1

The relationships of the detector's arms (dashed lines making an angle 2Ω), the detector's x-y axes (with the x-axis bisecting the angle between the arms), and the local compass directions (defining the angle of orientation α).

Figure 2

The relations among the detector's axes (x,y,z), the Earth's axes (x′,y′,z′) and the wave's axes (X,Y,Z). Here β and γ are the detector's latitude and longitude respectively, and α its orientation as in Fig. 1. The angles θ and ϕ give the incoming direction of the wave as measured with respect to the Earth's axes. The angle ψ determines the polarization angle of the wave.

Figure 3

Single-antenna detection probability as a function of the detector's thresholds X_s^M.

Figure 4

Parts (a-f) display contours of constant double-coincidence probability as functions of the detector's thresholds of various pairs of detectors. See the text for a full discussion.

References

Caves, C.M., 1981. Phys.Rev.D, 23, 1693

Clarke, J.P.A. & Eardly, D.M., 1977. Astrophys.J., 215, 311

Clarke, J.P.A., van den Heuvel, E.P.J. & Sutantyo, W., 1979. Astron.Astrophys., 72, 120

Dewy, D., 1986. in *Proceedings of the Fourth Marcel Grossmann Meeting on General Relativity*, ed. Ruffini, R. Elsevier

Fox, L. & Parker, I.B., 1968. *Chebyshev Polynomials in Numerical Analysis*, Oxford University Press

Hamming, R.W., 1973. *Numerical Methods for Scientists and Engineers*, McGraw-Hill, Kogekushe Ltd.

Hough, J., Meers, B.J., Newton, G.P., Robertson, N.A., Ward, H., Schutz, B.F., Drever, R.W.P., Tolcher, R. & Corbett, I.F., (1986) *A British Long Baseline Gravitational Wave Observatory*, Rutherford Appleton Laboratory Report GWD/RAL 86-001, Chilton, Oxon., U.K.

Schutz, B.F., 1986. Nature, 323, 310

Schutz, B.F. & Tinto, M., 1987. Mon.Not.R.astr.Soc., 224, 131

Shreider, Yu.A., 1966. *The Monte Carlo Method*, ed. Shreider, Yu.A., Oxford Pergamon

Thorne, K.S., 1987. In: *300 Years of Gravitation*, eds. Hawking, S.W. & Israel, W. Cambridge University Press

Tinto, M., 1987. Mon.Not.R.astr.Soc., to appear

Appendix

We provide here the coefficients of the linear fits to the single-antenna detection probability and the double, triple and quadruple coincidence rates for thresholds X_*^{H} in the interval [0, 0.5]. The fits themselves may be deduced by applying a least-squares method to a linear combination of Chebyshev's polynomials. Their formal expressions may be written as follows:

$$S(X_*^{H}) = \sum_{i=0}^{2} A_i \, T_i(X_*^{H}) \tag{A1}$$

$$C(X_{1*}^{H}; X_{2*}^{H}) = \sum_{i,j=0}^{2} B_{ij} \, T_i(X_{1*}^{H}) T_j(X_{2*}^{H}) \tag{A2}$$

$$C(X_{1*}^{H}; X_{2*}^{H}; X_{3*}^{H}) = \sum_{i,j,k=0}^{2} C_{ijk} \, T_i(X_{1*}^{H}) T_j(X_{2*}^{H}) T_k(X_{3*}^{H}) \tag{A3}$$

$$C(X_{1*}^{H}; X_{2*}^{H}; X_{3*}^{H}; X_{4*}^{H}) = \sum_{i,j,k,\ell=0}^{2} D_{ijk\ell} T_i(X_{1*}^{H}) T_j(X_{2*}^{H}) T_k(X_{3*}^{H}) T_\ell(X_{4*}^{H}) \tag{A4}$$

where the functions T are the 1st kind Chebyshev polynomials defined in the range (0,1), (Fox & Parker, 1968).

Since the coincidence probabilities are invariant by interchanging their arguments, we would expect symmetry in the coefficients B_{ij}, C_{ijk} and $D_{ijk\ell}$ under permutation of

the indices. However, because our data have been obtained by using a numerical method, we have seen that the symmetry in the coefficients is not exactly respected. By averaging the Chebyshev coefficients over permutations of the indices, we have verified that the accuracy of the fits is unchanged. Therefore we reproduce below only the symmetric parts of B_{ij}, C_{ijk} and D_{ijkl}.

CHEBYSHEV COEFFICIENTS FOR SINGLE-ANTENNA

A1= 0.3019E-01 A2=-0.1142E+01 A3=-0.1366E+00

CHEBYSHEV COEFFICIENTS FOR CALIFORNIA-MAINE BASELINE

B00= 0.2830E+00 B01= 0.4461E+00

B11= 0.2177E+01 B02= 0.2103E+00

B12= 0.5887E+00 B22= 0.2689E+00

CHEBYSHEV COEFFICIENTS FOR CALIFORNIA-SCOTLAND BASELINE

B00=-0.4849E-01 B01=-0.1186E+00

B11= 0.1181E+01 B02=-0.2719E-01

B12= 0.1404E+00 B22= 0.4249E-01

CHEBYSHEV COEFFICIENTS FOR CALIFORNIA-GERMANY BASELINE

B00=-0.6364E-01 B01=-0.1367E+00

B11= 0.1154E+01 B02=-0.3305E-01

B12= 0.1267E+00 B22= 0.3239E-01

CHEBYSHEV COEFFICIENTS FOR MAINE-SCOTLAND BASELINE

B00= 0.1417E+00 B01= 0.2030E+00

B11= 0.1756E+01 B02= 0.1032E+00

B12= 0.3990E+00 B22= 0.1776E+00

CHEBYSHEV COEFFICIENTS FOR MAINE-GERMANY BASELINE

B00= 0.8759E-02 B01=-0.1506E-01

B11= 0.1381E+01 B02= 0.1240E-01

B12= 0.2313E+00 B22= 0.9386E-01

CHEBYSHEV COEFFICIENTS FOR SCOTLAND-GERMANY BASELINE

B00= 0.7188E+00 B01= 0.1174E+01

B11= 0.3426E+01 B02= 0.5201E+00

B12= 0.1137E+01 B22= 0.5277E+00

CHEBYSHEV COEFFICIENTS FOR THE TRIPLE CALIFORNIA-MAINE-SCOTLAND

C000= 0.3400E-03 C001=-0.1404E+00 C011=-0.4347E+00

C111=-0.2857E+01 C002=-0.1061E-01 C012=-0.1113E+00

C112=-0.6781E+00 C022= 0.5822E-03 C122=-0.1892E+00

C222=-0.2154E-01

CHEBYSHEV COEFFICIENTS FOR THE TRIPLE CALIFORNIA-MAINE-GERMANY

C000=-0.9962E-02 C001=-0.9047E-01 C011=-0.2518E+00

C111=-0.2377E+01 C002=-0.6925E-03 C012=-0.5724E-01

C112=-0.5096E+00 C022= 0.1195E-01 C122=-0.1325E+00

C222=-0.7230E-02

CHEBYSHEV COEFFICIENTS FOR THE TRIPLE CALIFORNIA-SCOTLAND-GERMANY

C000= 0.3001E-01 C001=-0.1697E+00 C011=-0.6225E+00

C111=-0.3403E+01 C002= 0.1249E-01 C012=-0.1379E+00

C112=-0.8210E+00 C022= 0.1128E-01 C122=-0.2133E+00

C222=-0.1729E-01

CHEBYSHEV COEFFICIENTS FOR THE TRIPLE MAINE-SCOTLAND-GERMANY

C000= 0.2395E-01 C001=-0.2897E+00 C011=-0.9883E+00

C111=-0.4326E+01 C002=-0.1676E-01 C012=-0.2410E+00

C112=-0.1130E+01 C022=-0.4680E-02 C122=-0.3055E+00

C222=-0.2855E-01

CHEBYSHEV COEFFICIENTS FOR QUADRUPLE COINCIDENCES

D0000= 0.1981E+00 D0001= 0.3356E+00 D0011= 0.7951E+00D0111= 0.2047E+01

D1111= 0.7502E+01 D0002= 0.1565E+00 D0012= 0.2955E+00D0112= 0.6866E+00

D1112= 0.2198E+01 D0022= 0.1441E+00 D0122= 0.2639E+00D1122= 0.7453E+00

D0222= 0.1338E+00 D1222= 0.2832E+00 D2222= 0.1413E+00

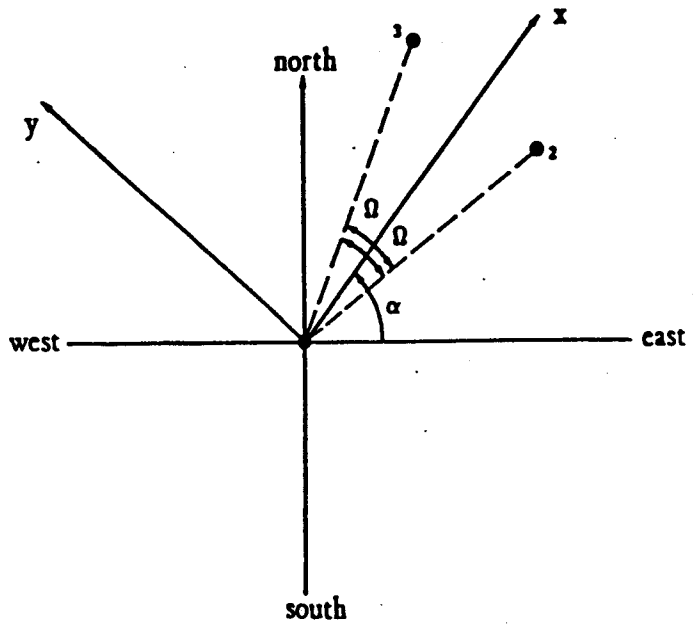

Figure 1.

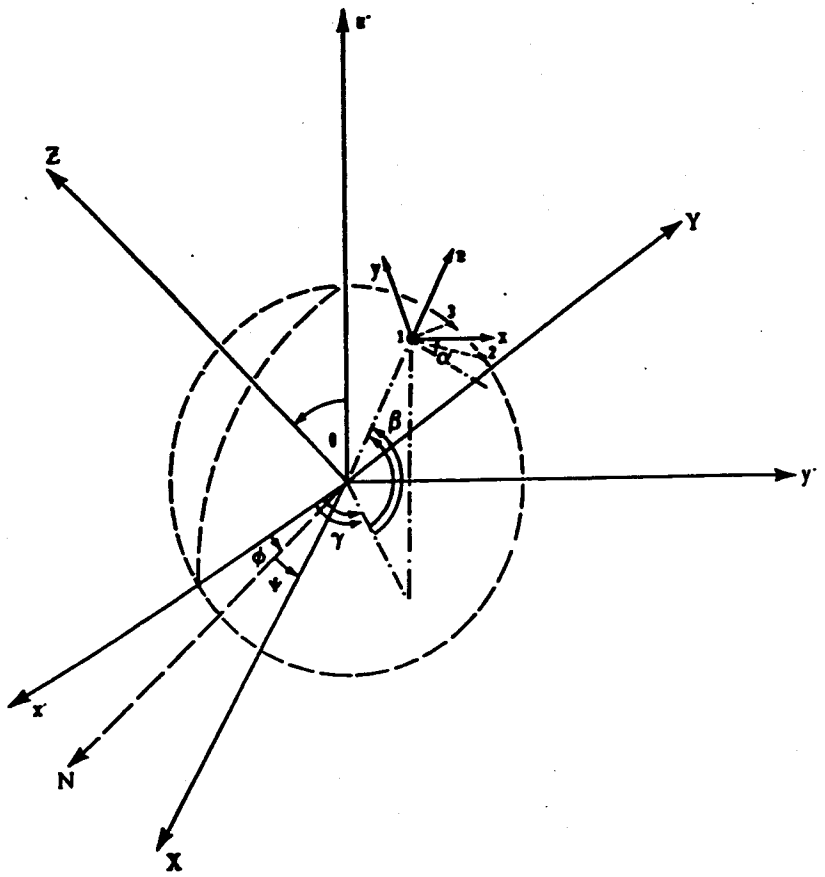

Figure 2.

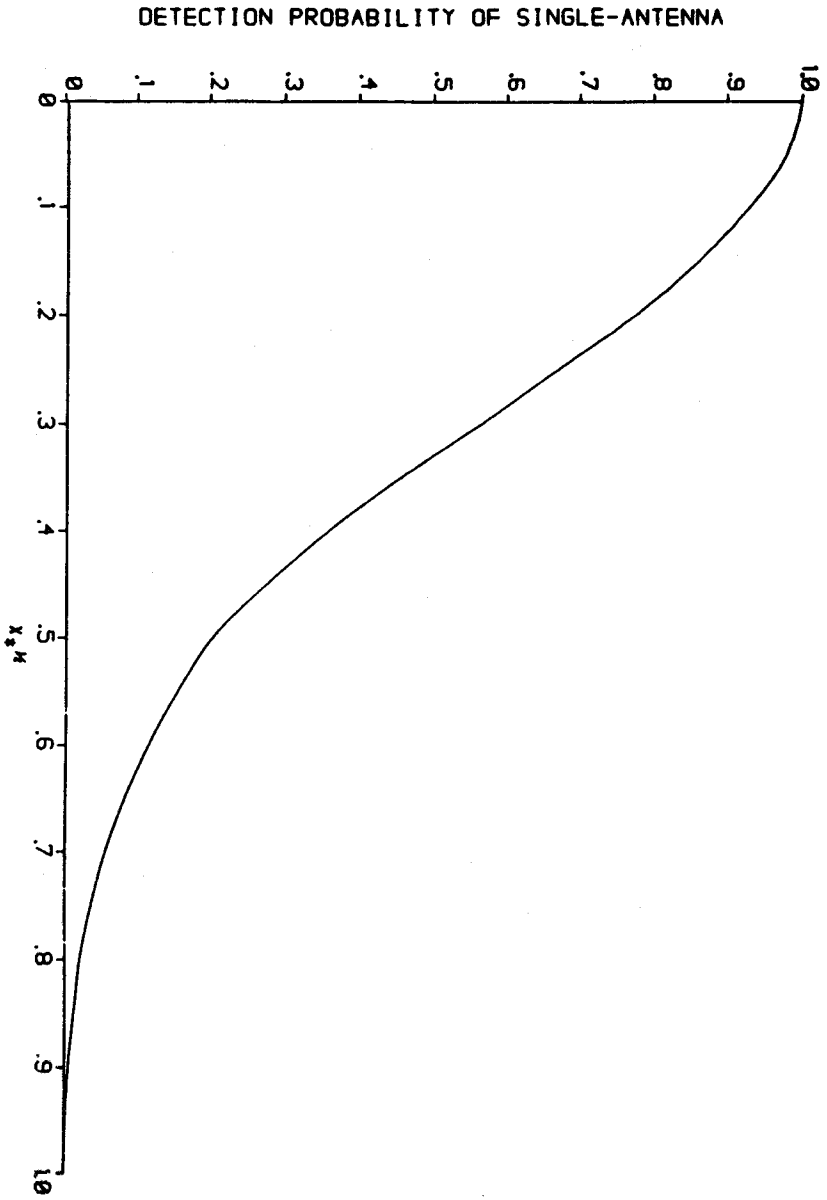

Figure 3

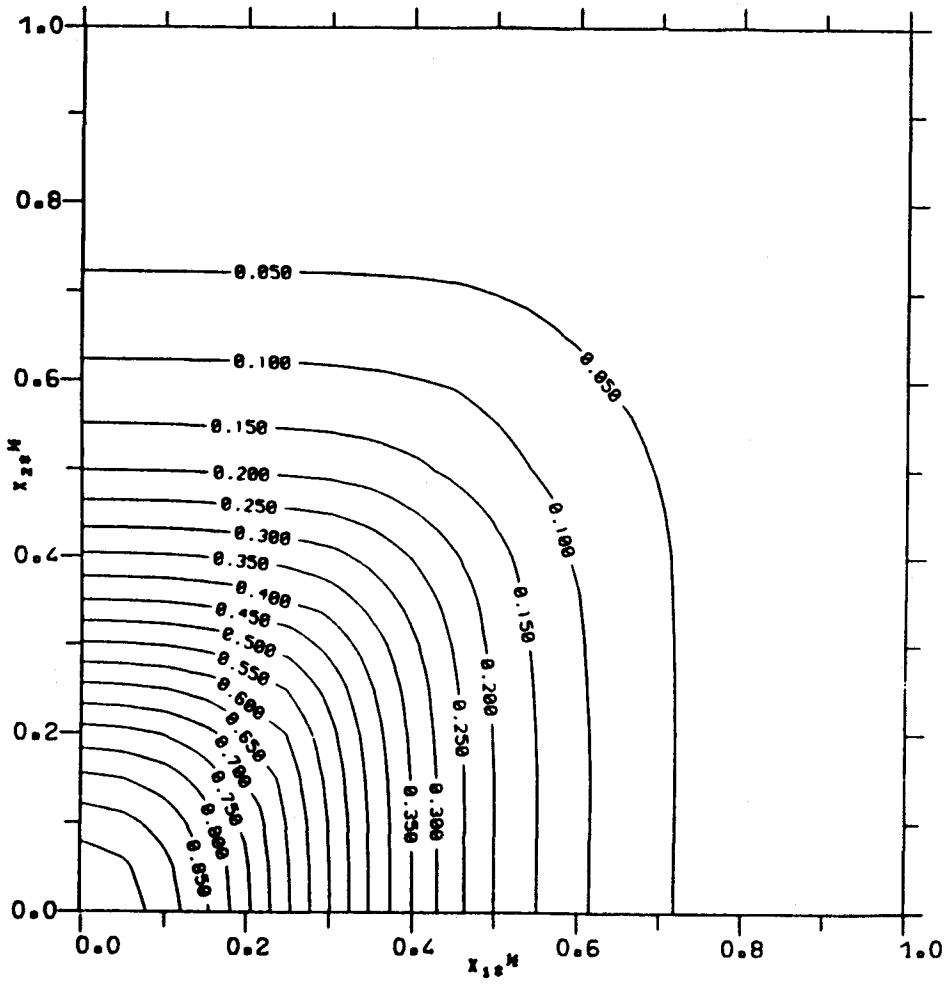

Figure 4(a)

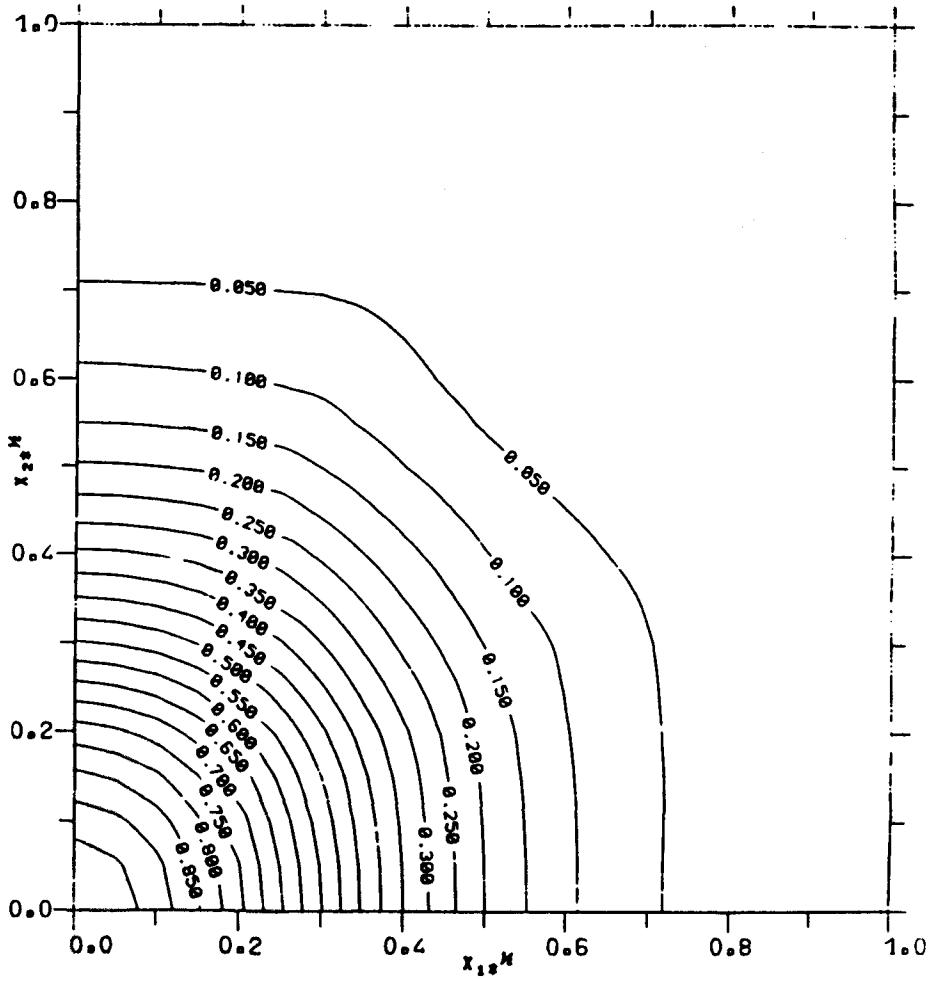

Figure 4(b)

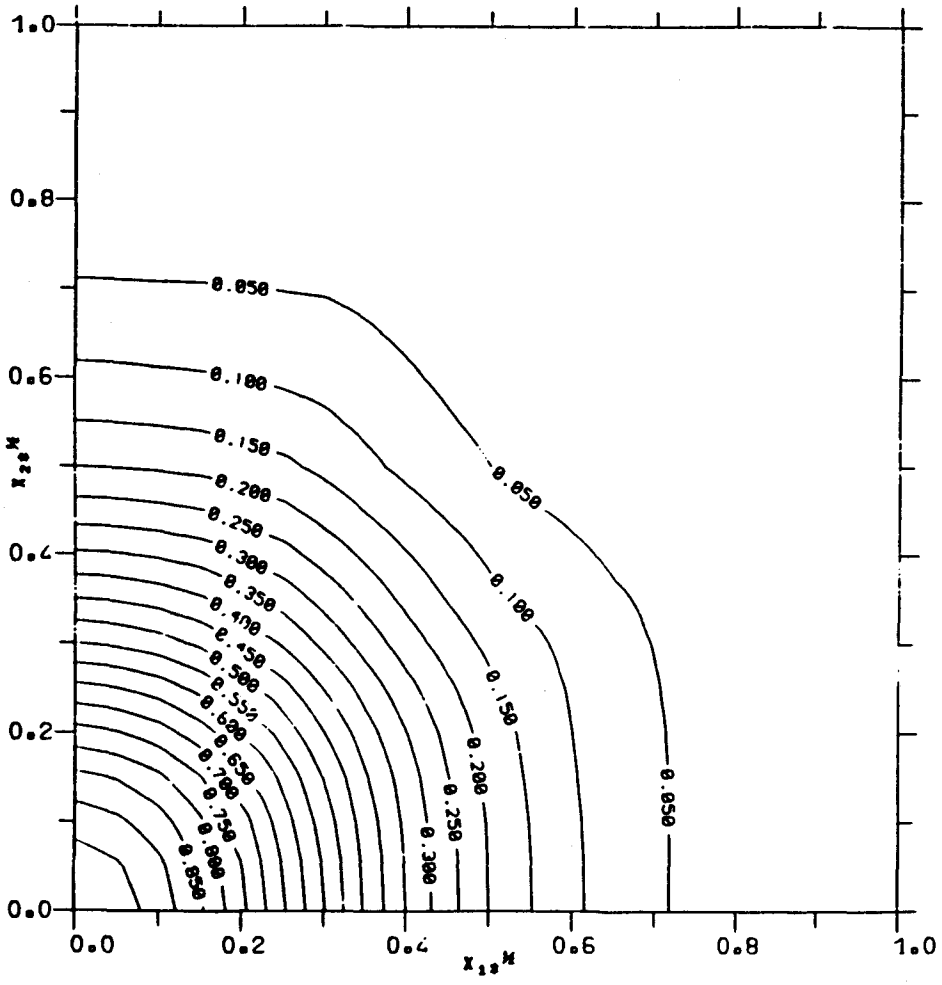

Figure 4(c)

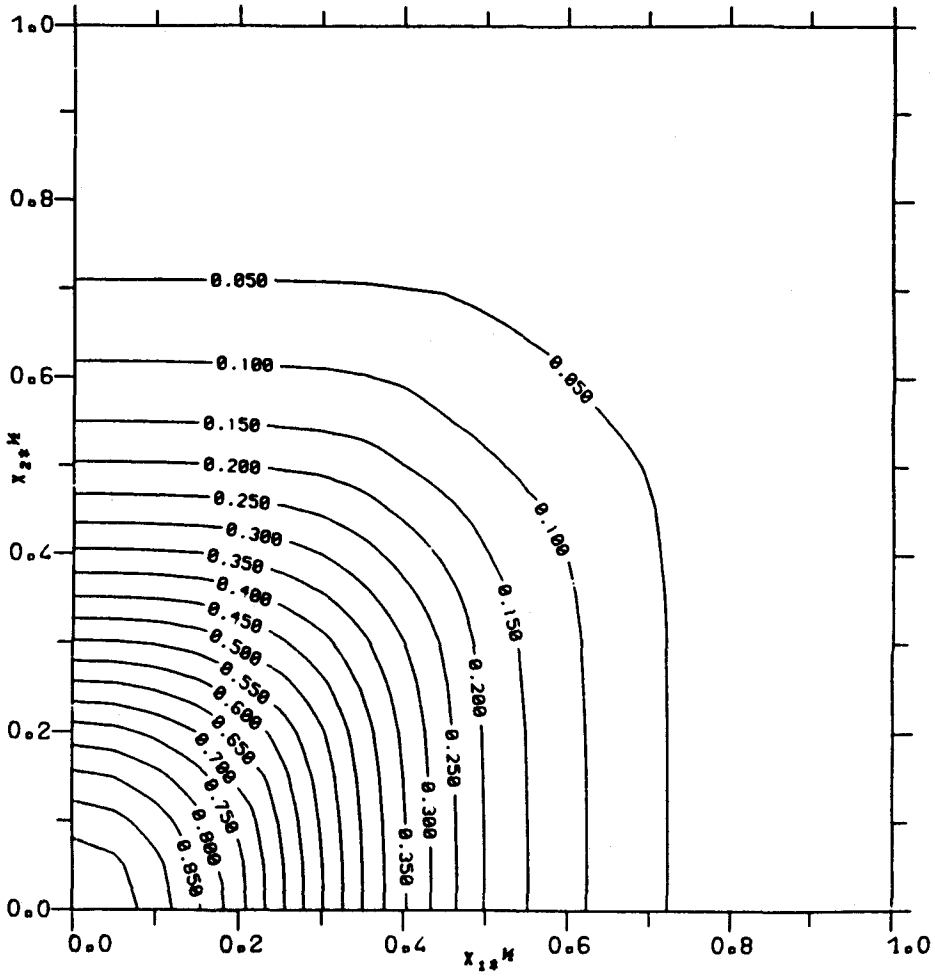

Figure 4(d)

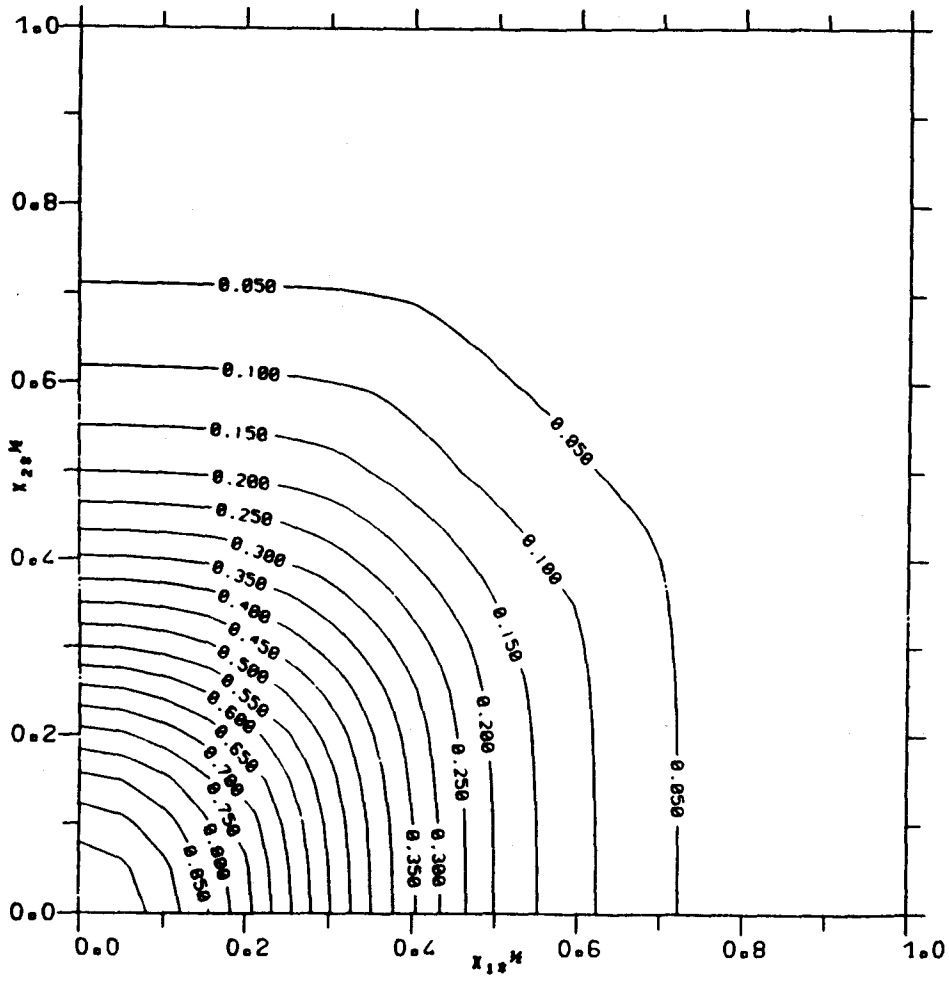

Figure 4(e)

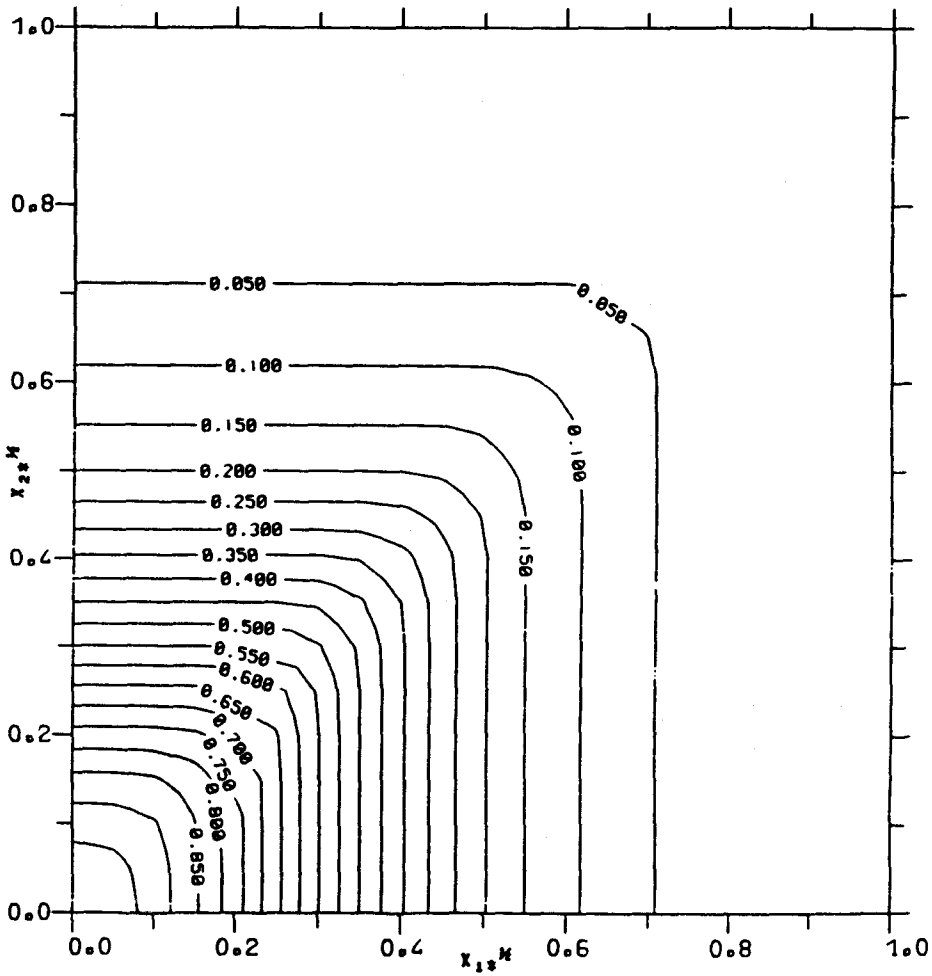

Figure 4(f)